IGNACE REVELL BATHOLITH LiDAR SURVEY

APM-REP-01332-0239 April 2019

ATLIS Geomatics Inc.

NUCLEAR WASTE MANAGEMENT ORGANIZATION
SOCIÉTÉ DE GESTION DES DÉCHETS NUCLÉAIRES

Nuclear Waste Management Organization
22 St. Clair Avenue East, 4th Floor
Toronto, Ontario
M4T 2S3
Canada

Tel: 416-934-9814
Web: www.nwmo.ca

ATLIS

FINAL REPORT

1674 – Ignace Revell Batholith LiDAR Survey

Nuclear Waste Management Organization

ATLIS Geomatics Inc.

1333 Dugald Road
Winnipeg, MB R2J 0H3
(204) 775-1211

#208 – 3016 19th Street NE
Calgary, AB T2E 6Y9
(403) 516-6066
www.atlisgeo.com

TABLE OF CONTENTS

1.0 PROJECT SUMMARY

This report documents the ground and aerial survey acquisition process for the Ignace Revell Batholith LiDAR Survey (Project number - 1674).

The ground survey was conducted by Andrew Brooker on October 11th, 2017 using a Leica GS14 RTK system and was processed by Jesse Mauch using Waypoint GrafNet.

The aerial survey was conducted by Michael Kettridge on October 11th, 2017 using a Leica ALS70-HP LiDAR sensor, Leica RCD30 metric camera and Leica IPAS CUS6 airborne GPS/IMU aboard a PA-31 Piper Navajo aircraft. The flight data was processed by Eric Gareau using NovAtel Inertial Explorer.

The LiDAR data was processed by Michael Kettridge using Terrasolid TerraMatch and TerraScan to calibrate and classify the data, respectively. The surface models generated from the LiDAR data were prepared by Neel Chooniedass using ESRI ArcGIS, the contours where generated in GeoCue LP360 by Michael Kettridge and the Hillshade model was generated in Blue Marble Geographic Global Mapper by Michael Kettridge.

The imagery data was recovered by Eric Gareau using Leica ImagePro, who also performed aerial triangulation analysis on the imagery using Trimble Inpho. Orthophoto production was contracted to Weaverbird Engineering & Technology and their work product was checked by Neel Chooniedass.

1.1 PROJECT DESCRIPTION

The Ignace Revell Batholith LiDAR Survey project was commissioned by Nuclear Waste Management Organization as part of it's commitment to implement Adaptive Phased Management (APM), Canada's plan for the long-term management of used nuclear fuel through the containment and isolation of used nuclear fuel in a deep geological repository in a suitable rock formation.

This project provides an accurate, high-resolution, bare-earth Digital Elevation Model (DEM) of the proposed area, which will serve as an important element of the Descriptive Geosphere Site Model and provide definitive surface boundary conditions for watershed-scale groundwater system analysis, in direct support of assessing technical site suitability, repository design and layout and possibilities for development of a strong repository safety case.

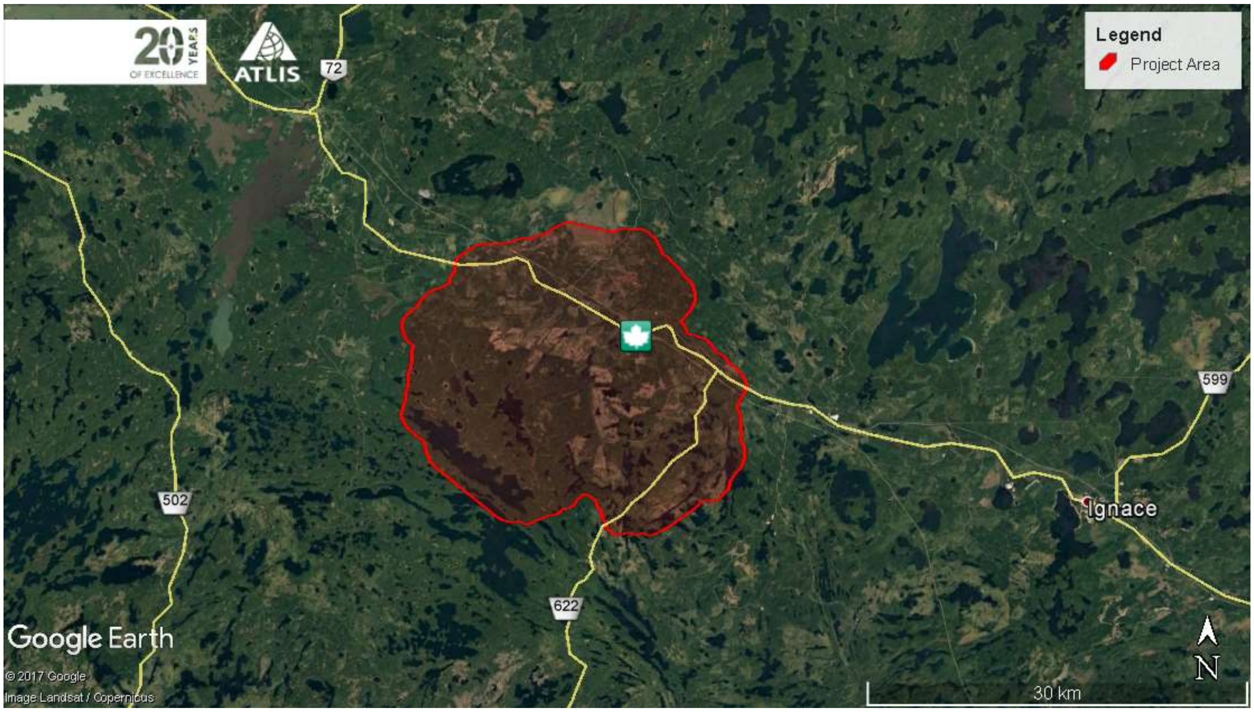

Figure 1: Project Area

1.2 COORDINATE SYSTEM

Deliverables for this project have been generated using the coordinate systems specified in *Table 1*

Horizontal Reference Frame (epoch)	NAD83 (CSRS) (2010.0)
Vertical Reference Frame (Geoid Model)	CGVD2013 (CGG2013)
Ellipsoid	GRS80
Coordinate System (Zone)	UTM (Z15N)
Units	Metric

Table 1: Project Coordinate System

1.3 ACCURACY STATEMENT

This data set was tested to meet ASPRS Positional Accuracy Standards for Digital Geospatial Data (2014) for a 4cm RMSEx / RMSEy Horizontal Accuracy Class. Actual positional accuracy was found to be RMSEx = 58mm and RMSEy = 9mm which equates to Positional Horizontal Accuracy = +/-82mm at 95% confidence level.

This data set was tested to meet ASPRS Positional Accuracy Standards for Digital Geospatial Data (2014) for a 3cm RMSEz Vertical Accuracy Class. Actual NVA accuracy was found to be RMSEz = 25mm, equating to +/-49mm at 95% confidence level. Actual VVA accuracy was found to be unknown at the 95th percentile.

2.0 GROUND SURVEY

The ground survey for this project was conducted by Andrew Brooker on October 11, 2017 using two Leica GS14 GNSS receivers configured for RTK and static observations. ATLIS utilized High Precision 3D monument 66D8147, with coordinates published by NRCan, as the primary reference monument for georeferencing the ground survey for this project. ATLIS surveyed published benchmark 90U176 as a vertical check on the survey.

Calibration points for the aerial survey were collected using a mix of RTK and static GNSS observations. ATLIS was only able to survey 13 ground control points for this project due to limited site accessibility, particularly in the south west corner of the project. RTK observations were processed by Andrew Brooker using Leica SurveyPro and static GNSS observation were processed by Jesse Mauch using Waypoint GrafNet, with processing results derived from the NRCan PPP service to serve as a check.

2.1 PRIMARY CONTROL

ATLIS used monument 66D8147 as the primary control monument for conducting both the RTK and static GNSS portions of the ground survey for this project. ATLIS used the published, geographic coordinates from NRCan's Passive Control Network website for monument 66D8147 as the RTK base station coordinates and as the control coordinates when processing the static GNSS network, as presented in *Table 2*.

ATLIS observed monument 66D8147 for 7h 34m and 56s using a Leica GS14 dual-frequency GNSS receiver recording at 1Hz. ATLIS processed the static observation using the PPP Service offered by NRCan after the required seven days had passed, resulting in a PPP solution with 95% sigma values of 0.003m, 0.006m and 0.013m for the latitude, longitude and ellipsoid height, respectively.

The residuals between the published UTM coordinates and those computed by GrafNet and PPP are presented in *Table 3*. The results of *Table 3* demonstrate the control tolerance criteria for the ground control meets the acceptance standard of ±15cm Vertical and ±30cm Horizontal.

ATLIS was unable to survey the required control monument 00819970048, due to safety issues arising from the inaccessibility of the monument.

	LATITUDE	LONGITUDE	ELLIPSOID HEIGHT
66D8147	49° 35′ 04.02189″ N	92° 15′ 50.10574″ W	371.201

Table 2: Primary Control Monument Geographic Coordinates

66D8147	NORTHING	ΔN	EASTING	ΔE	ELEVATION	ΔZ
Published	5492689.894	-	553205.890	-	403.398	-
GrafNet	5492689.895	0.001	553205.890	0.000	403.396	-0.002
PPP	5492689.891	-0.003	553205.889	-0.001	403.403	0.005

Table 3: UTM Coordinates for Primary Control Monument

2.2 BENCHMARKS

ATLIS collected static observations on Primary Vertical Control monument 90U176 for 10m and 57s using a Leica GS14 dual-frequency GNSS receiver recording at 1Hz to provide a check on the survey results. ATLIS processed the static observation using the PPP service offered by NRCan after the required seven days had passed, resulting in a PPP solution with 95% sigma values of 0.341m, 0.679m and 0.726m for the latitude, longitude and ellipsoid height coordinates, respectively.

The resulting residuals between the published and derived coordinates for 90U176 are shown in *Table 4*. The large horizontal residuals on 90U176 are the result of the low positional accuracy of the monument, for which the horizontal coordinates have been obtained via scaling from a topographic map. The large vertical residual on the PPP solution fall within the 95% sigma value of 0.726m for the PPP solution.

The results of *Table 4* demonstrate the control tolerance criteria for the ground control meets the acceptance standard of ±15cm Vertical, however the horizontal criteria could not be verified.

90U176	NORTHING	ΔN	EASTING	ΔE	ELEVATION	ΔZ
Published	5475852.365		563734.028		476.322	
GrafNet	5475984.992	132.627	563673.311	-60.717	476.280	-0.042
PPP	5475984.947	132.582	563673.144	-60.884	475.644	-0.678

Table 4: Check Monument Residuals

2.3 STATIC DATA PROCESSING

ATLIS processed all the static GNSS observations collected for this project in GrafNet using monument 66D8147 as a fixed control point. All the baselines were processed using Forward/Reverse processing and with an elevation mask of 15°. GrafNet was able to successfully process each baseline with a Fixed ARTK solution. ARTK stands for Advance RTK and is a NovAtel RTK engine used to resolve integer carrier phase ambiguities for rapid centimeter-level positioning for short baseline, open sky, dual frequency data.

Final coordinates for each station were computed using a traverse solution from 66D8147 in GrafNet.

NAME	LENGTH (hh:mm:ss)	DIST(km)	RMS(mm)	σ(mm)
66D8147 to 90U176	0:10:57	19.722	5.3	32.8
66D8147 to RTKVERT010	0:08:00	20.471	4	24
66D8147 to RTKVERT020	0:03:09	1.223	3.3	22
66D8147 to RTKVERT1006	0:03:01	18.974	0	28.4
66D8147 to STATIC001	0:07:18	17.271	0	21.7
66D8147 to STATIC002	0:07:45	20.239	2	27.8
66D8147 to STATIC1006	0:14:06	16.934	3.2	33.1
66D8147 to VERT1001	0:11:11	20.54	3.2	25.8
66D8147 to VERT1002	0:09:32	21.148	8	28.7
66D8147 to VERT1003	0:09:29	19.964	4.7	23.8
66D8147 to VERT1004	0:09:59	19.692	0	22.9
66D8147 to VERT1005	0:09:34	18.493	2	42.3
66D8147 to VERT1007	0:10:11	17.319	0	22.3
66D8147 to VERT1008	0:10:32	18.233	4	23

Table 5: Static Baseline Processing Results

STATION	LATITUDE	LONGITUDE	ELL. HEIGHT
66D8147	49°35′04.02189″ N	92°15′50.10574″ W	371.201
90U176	49°25′59.51706″ N	92°07′18.53758″ W	443.899
RTKVERT010	49°24′53.69996″ N	92°09′14.15664″ W	435.548
RTKVERT020	49°35′18.21215″ N	92°16′46.96396″ W	363.656
RTKVERT1006	49°30′01.52500″ N	92°02′08.80715″ W	412.253
STATIC001	49°30′24.78730″ N	92°03′25.87530″ W	394.251
STATIC002	49°25′13.12610″ N	92°08′35.92550″ W	420.289
STATIC1006	49°30′12.37199″ N	92°03′56.97441″ W	402.612
VERT1001	49°24′51.78568″ N	92°09′12.25025″ W	433.215
VERT1002	49°24′11.36944″ N	92°10′33.33453″ W	416.593
VERT1003	49°25′40.81924″ N	92°07′43.69288″ W	443.426
VERT1004	49°26′01.30052″ N	92°07′16.96112″ W	443.079
VERT1005	49°28′03.67058″ N	92°04′55.50317″ W	426.734
VERT1007	49°30′23.68208″ N	92°03′24.11846″ W	394.3
VERT1008	49°30′11.08711″ N	92°02′42.80273″ W	396.492

Table 6: Geographic Coordinate Traverse Results

STATION	EASTING	NORTHING	ELEVATION
66D8147	553205.9	5492690	403.396
90U176	563673.3	5475985	476.28
RTKVERT010	561367.5	5473926	467.877
RTKVERT020	552060.1	5493117	395.812
RTKVERT1006	569815.7	5483535	444.798
STATIC001	568256.7	5484233	426.768
STATIC002	562131	5474534	452.636
STATIC1006	567636.1	5483842	435.111
VERT1001	561406.6	5473867	465.544
VERT1002	559786.5	5472601	448.882
VERT1003	563173.3	5475402	475.796
VERT1004	563704.4	5476040	475.461
VERT1005	566507.4	5479853	459.182
VERT1007	568292.5	5484200	426.818
VERT1008	569128.3	5483821	429.024

Table 7: Grid Coordinate Traverse Results

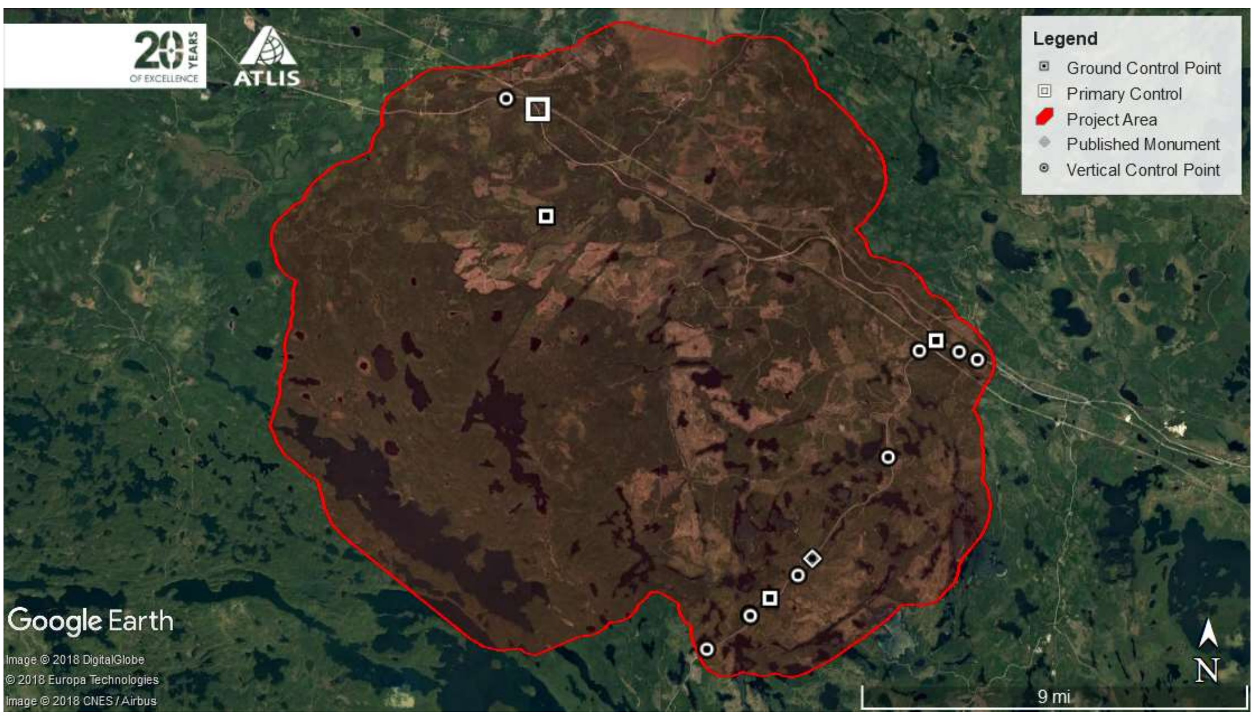

Figure 2: Ground Control Locations

3.0 AERIAL SURVEY

3.1 SENSOR CALIBRATION

ATLIS last performed a full-system calibration of the aerial sensor platform on May 14, 2017 over Selkirk, MB. The mission was successfully processed with only minor deviations from the previous calibration. The aerial sensor platform had remained in the aircraft, unaltered, at the time this project was acquired.

3.2 ACQUISITION

The aerial survey was conducted using a single lift, collecting both LiDAR data and imagery simultaneously, on October 11th, 2017, using a Piper Navajo PA-31 aircraft, piloted by Derek Anderson. The aircraft was equipped with a Leica ALS70 LiDAR sensor, Leica RCD30 metric camera and Leica IPAS-CUS6 flight management system, operated by Michael Kettridge. ATLIS performed a KAR-turn over Monument 66D8147 at the beginning and end of the flight to help initialize the airborne GNSS and performed a cross line before the final KAR turn to aid the processing in producing a more reliable result.

The aerial survey flight plan was created in Leica MissionPro by Daniel Brooker to produce 15cm resolution imagery and 8ppsm (pulses per square metre) pulse density using a 50° field of view, 327kHz pulse rate and 47Hz scan rate on the scanner. The mission was designed to produce a 50% lateral overlap in between both the LiDAR swathes and the image frames.

The maximum baseline length encounter during the aerial survey was 47.56km at the airport; however, the maximum baseline length while online was 28.8km, which meets the maximum 30km baseline length specification for the project.

Aerial data acquisition began at 15:47 UTC and ended at 20:47 UTC. *Figure 4* shows the estimated solar angle during the acquisition window, with a solar angle of 27° at the beginning of the acquisition window, a maximum angle of 33° 18:00 UTC and 22° at the end of the acquisition window.

ATLIS encountered high, thin scattered clouds at the time of survey, but deemed the conditions suitable for conducting the aerial survey. ATLIS found the ground conditions at the time of survey to be free of snow, haze, smoke and dust and without signs of unusual flooding or inundation. ATLIS re-flew one of the mission due to missing frames discovered while on-mission, all remaining flight lines were found to have been successfully acquired without data voids or any system malfunctions.

Table 8 lists the mission specifications used to conduct the aerial survey. *Figure 3* shows the as-flown flight path used to conduct the aerial survey for this project.

Above Ground Level	1550m	**Scan Rate**	47Hz
Airspeed	150kts	**Pulse Rate**	327kHz
Lateral Overlap	50%	**Scanner Field of View**	50°
Forward Overlap	60%	**Laser Power**	100%

Table 8: Mission Specifications

Figure 3: Flight Paths

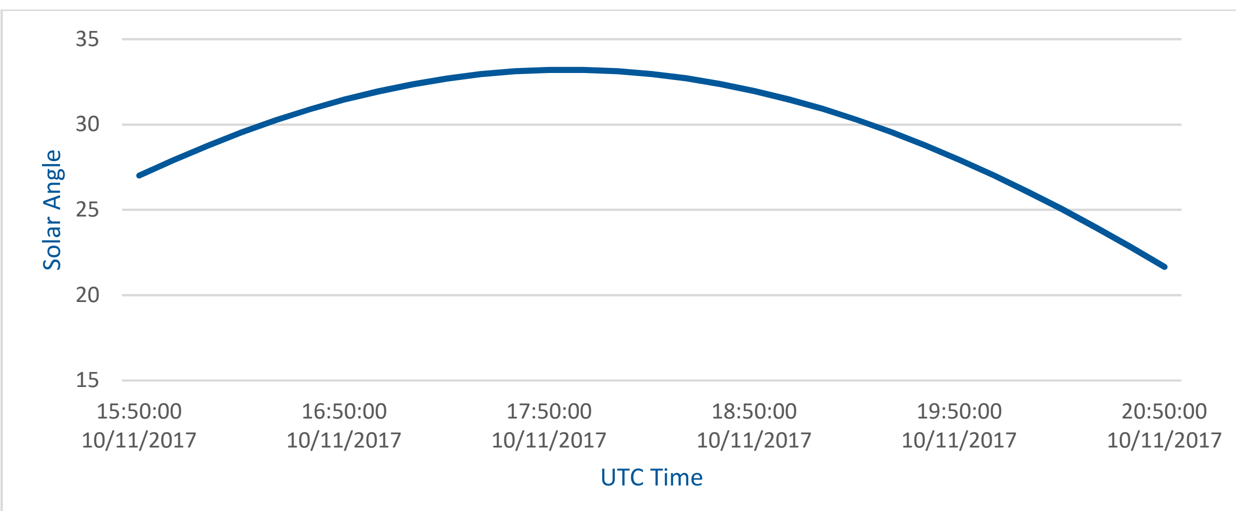

Figure 4: Solar Angle during Acquisition

3.3 FLIGHT PROCESSING

The airborne GNSS and INS data was processed by Eric Gareau using NovAtel Inertial Explorer to perform loosely-coupled, forward/reverse processing with smoothing to produce a Smoothed Best Estimate of Trajectory (SBET). The flight data was processed using static data collected on 66D8147 concurrently with the aerial survey and supplemented with 5-second precise ephemeris data. *Table 9* summarizes the critical flight processing statistics for this project.

	SATELLITE COUNT (ALL)	PDOP	HEIGHT PROFILE (B/W 15:47 AND 20:47)	HORIZONTAL DISTANCE SEPARATION	ESTIMATED POSITION ACCURACY (TRACE)	ESTIMATED ATTITUDE ACCURACY (ARCMIN)(3D)	COMBINED SOLUTION (3D)
Std.	1.088	0.128	12.80	7.869	0.00039	0.0238	0.00060
RMS	14.136	1.169	1958.51	16.858	0.00683	0.2091	0.00067
Avg.	14.094	1.162	1958.47	14.909	0.00682	0.2077	0.00030
Max.	16	2.020	2012.47	47.560	0.01302	0.3705	0.01840
Min.	10	0.880	1910.30	0.320	0.00612	0.1522	0.00000
Range	**Samples**						
0.050	-	-	-	-	40,449	0	40,449
0.100	-	-	-	-	0	0	0
0.150	-	-	-	-	0	0	0
0.250	-	-	-	-	0	39,783	0
0.500	-	-	-	-	0	666	0

Table 9: Flight Statistics

The X-axis of each plot in this section is expressed in GPS time.

SATELLITE COUNT

The Satellite Count Plot, shown in

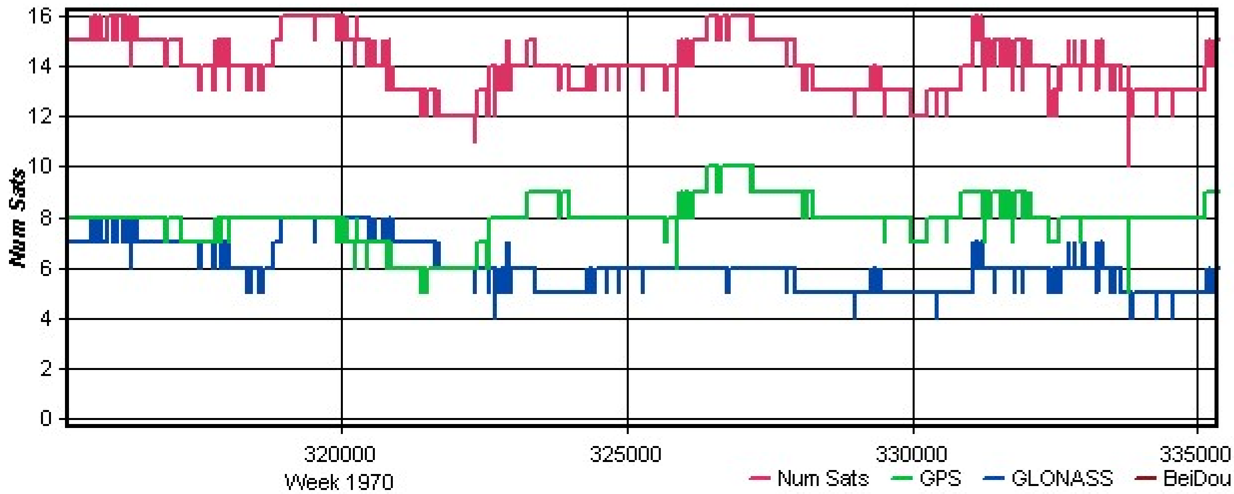

Figure 5, shows the number of satellites, broken down by constellation, being tracked by both the aircraft and static reference station at any given time throughout the acquisition window. In *Guidelines for RTK/RTN GNSS Surveying in Canada July 2013, version 1.1*, published by Natural Resources Canada, it states that a minimum of six GNSS satellites are required for a RTK/RTN solution; the minimum of ten satellites tracked for during this project meets the required standards for a quality GNSS solution.

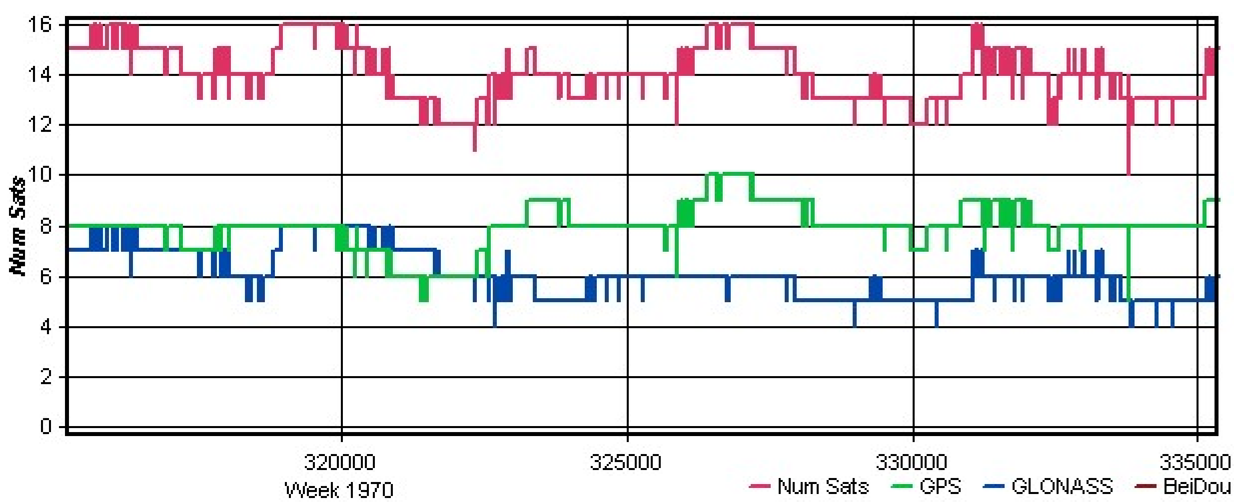

Figure 5: Satellite Count Plot

PDOP

Positional Dilution of Precision (PDOP) is a unitless measure of the satellite geometry relative to the GNSS receiver, in this case the aircraft GNSS antenna. PDOP is an important indicator in assessing the quality of a GNSS solution and a PDOP less than 3 is indicative of a strong GNSS positioning solution. The maximum

PDOP value of 2.020 experienced during this project meets the required standards for a quality GNSS solution.

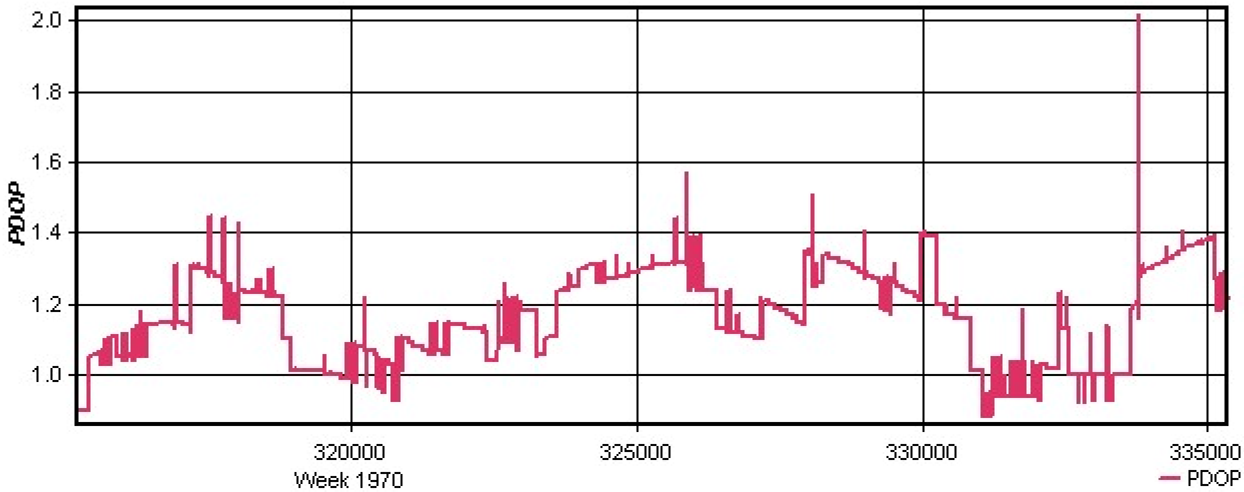

Figure 6: PDOP Plot

HEIGHT PROFILE

The Height Profile Plot, shown in

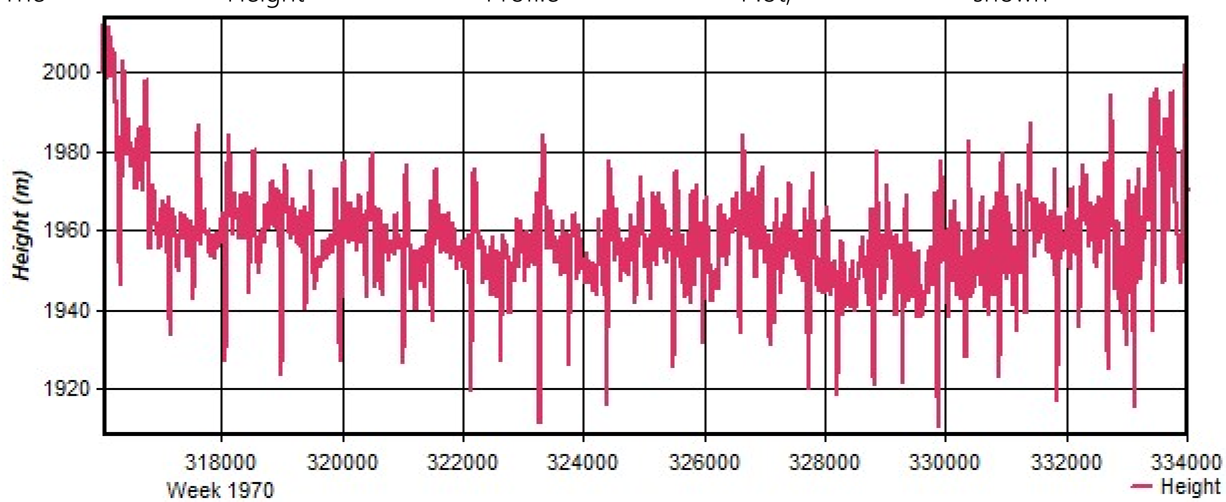

Figure 7, shows the altitude of the aircraft from 15:47 UTC to 20:47 UTC, while the aircraft was acquiring data. The time range for the plot and the associated statistics in *Table 9* have been limited to the acquisition window to avoid skewing the statistics with times before and after acquisition. The low standard deviation in the height profile, as seen in *Table 9* indicates a quality aerial survey acquisition process as changes in height effect the resolution of the imagery and the density of the LiDAR point cloud.

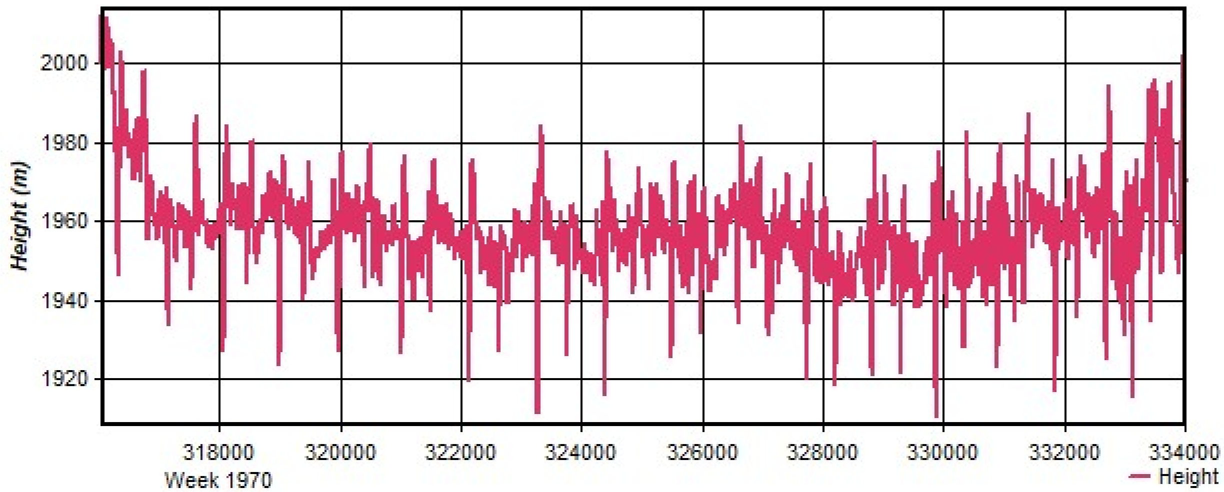

Figure 7: Height Profile Plot

HORIZONTAL DISTANCE SEPERATION

The Horizontal Distance Separation Plot, shown in *Figure 8*, shows the horizontal distance between the aircraft and the static reference station used to process the GNSS baselines. The plot shows that baselines were kept under the maximum 30km requirement, except during demobilization back to the airbase.

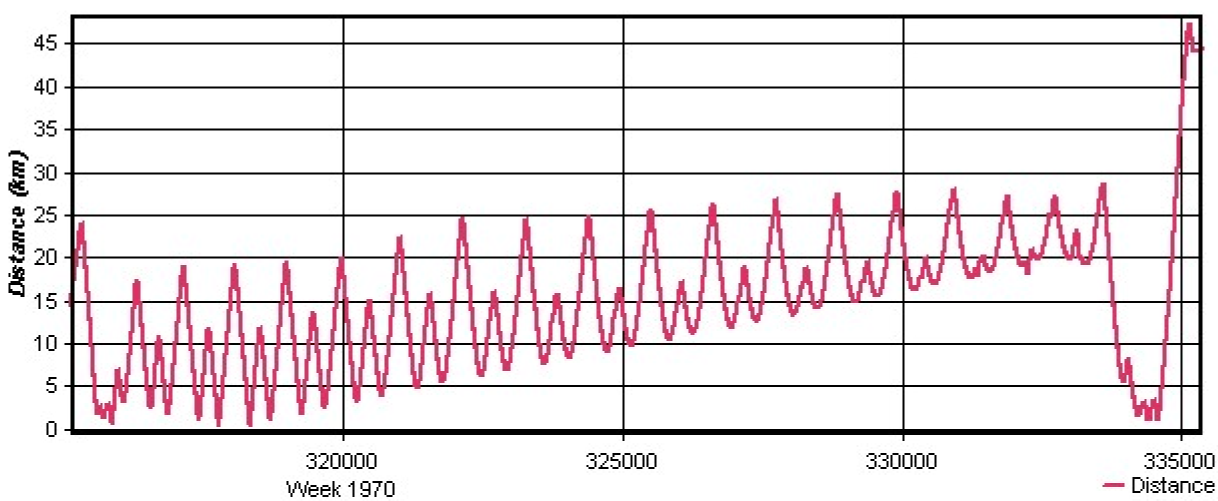

Figure 8: Horizontal Distance Separation Plot

ESTIMATED POSITION ACCURACY

The Estimated Position Accuracy plot, shown in *Figure 9*, shows the standard deviation computed in the GNSS/INS Kalman filter in terms of Northing, Easting and Height, with the Trace value representing the 3D combination of the positioning values. This plot serves to show the health of the GNSS component of the trajectory solution. The plot shows that the position component of the trajectory solution meets the quality standards of this project.

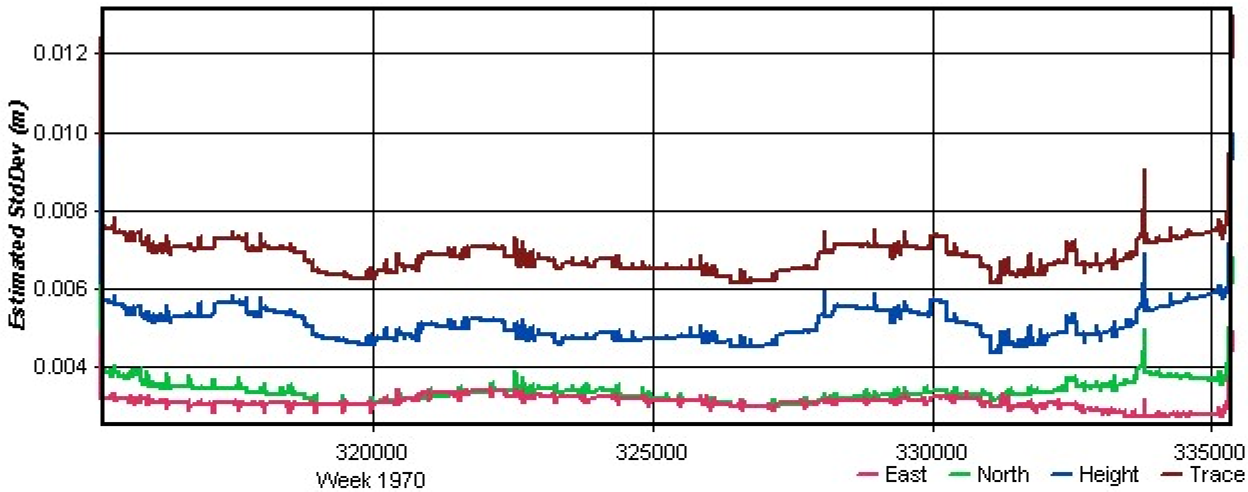

Figure 9: Estimated Position Accuracy Plot

ESTIMATED ATTITUDE ACCURACY

The Estimated Attitude Accuracy plot, shown in

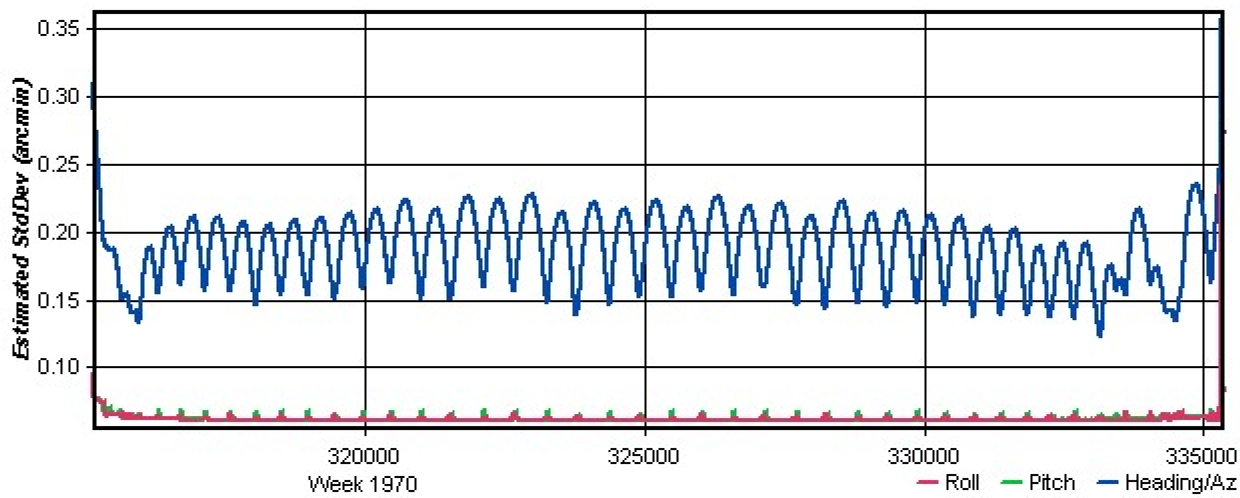

Figure 10, shows the standard deviation computed in the GNSS/INS Kalman filter in terms of roll, pitch and heading. This plot serves to show the health of the IMU component of the trajectory solution. The 3D values presented in *Table 9* combines each of the 3 attitude components into a single 3D value. The plot shows that the attitude component of the trajectory solution meets the quality standards of this project.

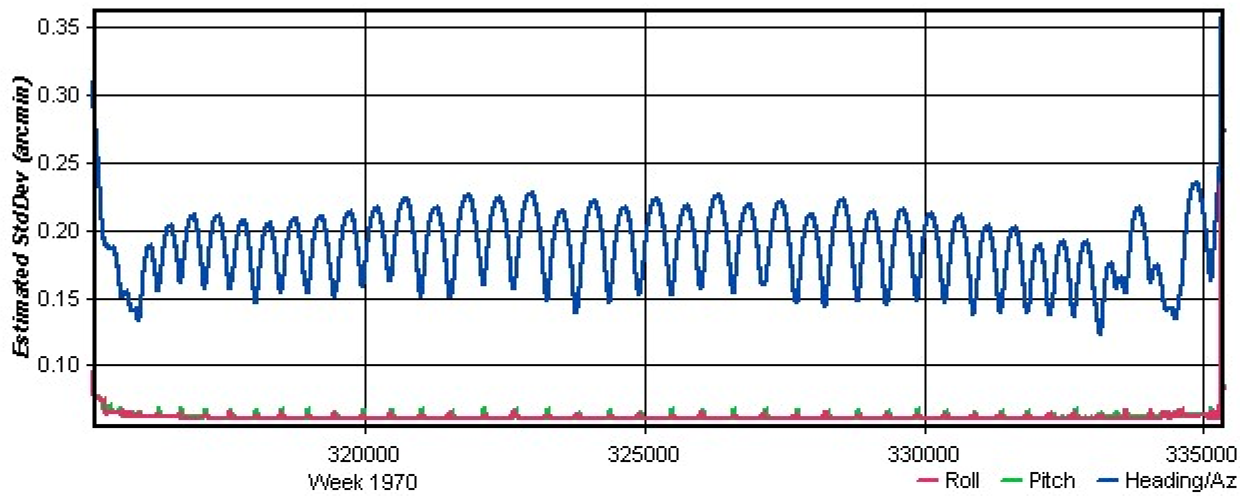

Figure 10: Estimated Attitude Accuracy Plot

COMBINED SEPARATION

The Combined Separation Plot, shown in *Figure 11*, shows the positioning difference between the forward and reverse solutions for the trajectory. The low values shown in this plot indicate that the carrier phase ambiguities have been correctly determined in both processing directions.

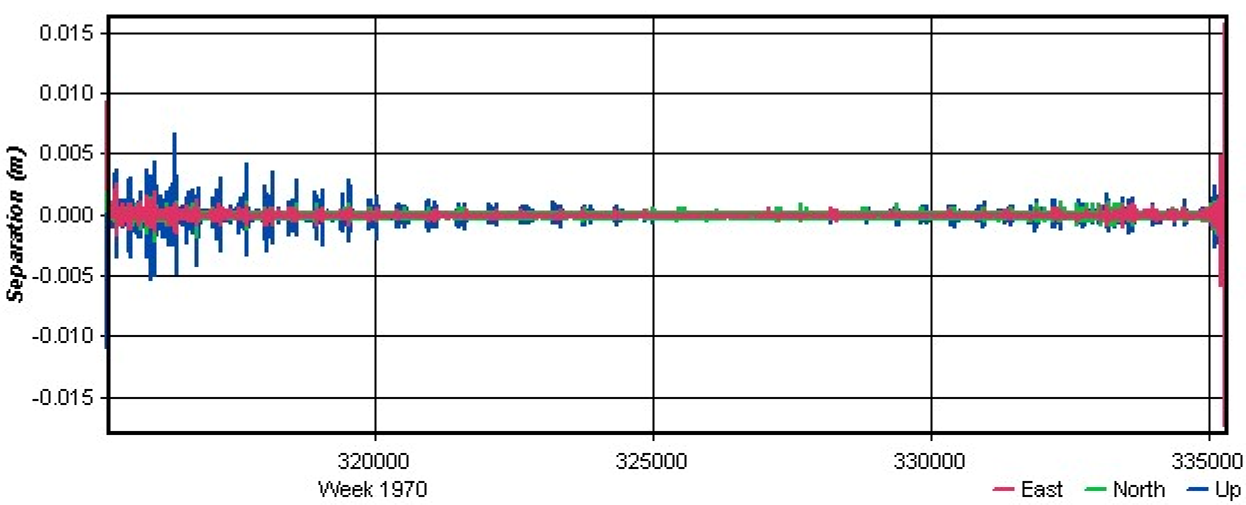

Figure 11: Combined Separation Plot

4.0 LIDAR PROCESSING

The processing of the LiDAR data was performed by Michael Kettridge using Terrasolid to calibrate, classify and tile the LiDAR data. The processed LiDAR data was used to generate a bare-earth DEM along with a first-return DSM (Digital Surface Model), each with a 1m resolution. ATLIS tiled the DEM, DSM and point cloud data into 1000m x 1000m tiles. The tiles were saved as ASCII and XYZ files for the DEM and DSM and as LAS v1.4 for the point cloud; each tile was named according to the UTM coordinate in the southwest corner of the tile.

4.1 RELATIVE CALIBRATION

ATLIS calibrated the 34 lines of the LiDAR data collected for this project using ground surface matching in Terrasolid TerraMatch, producing an average magnitude of 0.085m. Magnitude is a measure of the absolute elevation difference between the strip and a mean surface.

Table 10 summarizes the results of the relative calibration adjustment.

	AVERAGE	RMS	MINIMUM	MAXIMUM
# of Points	1793921	-	378104	2401488
Magnitude	0.085	0.086	0.069	0.109
Dz	0.000	0.004	-0.015	0.005

Table 10: Relative Adjustment Summary

4.2 ABSOLUTE CALIBRATION

Absolute calibration of the LiDAR data was carried out using 11 of the 13 check points observed for this project. The 2 points that were removed from the calibration were removed due to field survey error.

POINT	POINT ELEV.	LIDAR ELEV	ΔZ (LIDAR – CHECK)
RTKVERT010	467.513	Removed (blunder)	-
RTKVERT020	395.115	Removed (blunder)	-
RTKVERT1006	444.731	444.740	0.009
STATIC001	426.406	426.440	0.034
STATIC002	452.274	452.300	0.026
STATIC1006	434.749	434.750	0.001
VERT1001	465.182	465.170	-0.012
VERT1002	448.520	448.480	-0.04
VERT1003	475.434	475.420	-0.014
VERT1004	475.099	475.080	-0.019
VERT1005	458.820	458.780	-0.04
VERT1007	426.456	426.490	0.034
VERT1008	428.662	428.650	-0.012

Table 11: Vertical Control Results

Table 12 summarizes the statistics resulting from calibrating the LiDAR to the survey check points.

Average dZ	-0.003
Minimum dZ	-0.040
Maximum dZ	0.034
Average Magnitude	0.022
Root Mean Square	0.025
Standard Deviation	0.026

Table 12: Absolute Calibration Statistics

4.3 VALIDATION

Based on the results presented in *Table 12*, ATLIS concluded that the Non-Vegetation Accuracy (NVA) of the LiDAR data at the 95% confidence level was 49mm.

ATLIS analyzed the calibrated LiDAR to search for any data voids in the LiDAR data greater than or equal to four times the square of the Nominal Pulse Spacing of 0.57m, which translates into a pulse density of approximately 3ppsm. ATLIS ran a program with TerraScan to search for areas with a pulse density less than 3ppsm within a 2m grid, which produced 33,615 areas measuring a total of 49.5km^2. A visual inspection of the results, found that all void areas greater than 1000m^2 where over water, except for some patches along the northern and southern most sections of the project where there was not redundant overlap in the LiDAR data. Scattered void areas where noted between flight lines where slivering occurred due to a drop in lateral overlap caused by fluctuations in the terrain. No void areas were noted that were the result of a system error. *Figure 12* shows a histogram breakdown of the void areas by area and *Figure 13* shows the distribution of the void areas over the project area.

Testing of the spatial distribution of the LiDAR data showed an average pulse density of 8.2ppsm over the entire project area and 9.9ppsm when water bodies are removed. *Figure 14* shows the pulse density of the LiDAR data as a heat map, based on a 50m grid sampling.

Based on the QA/QC validation process, ATLIS determined that no re-flights were required for this project.

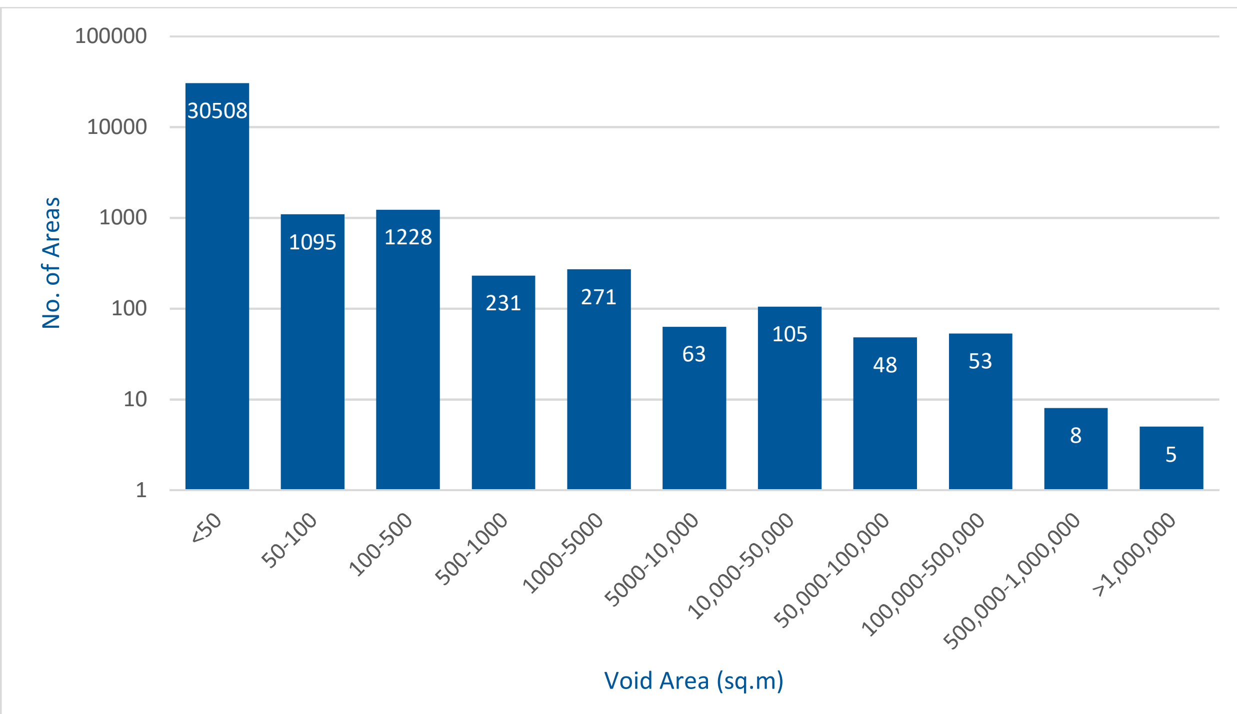

Figure 12: Void Area Histogram

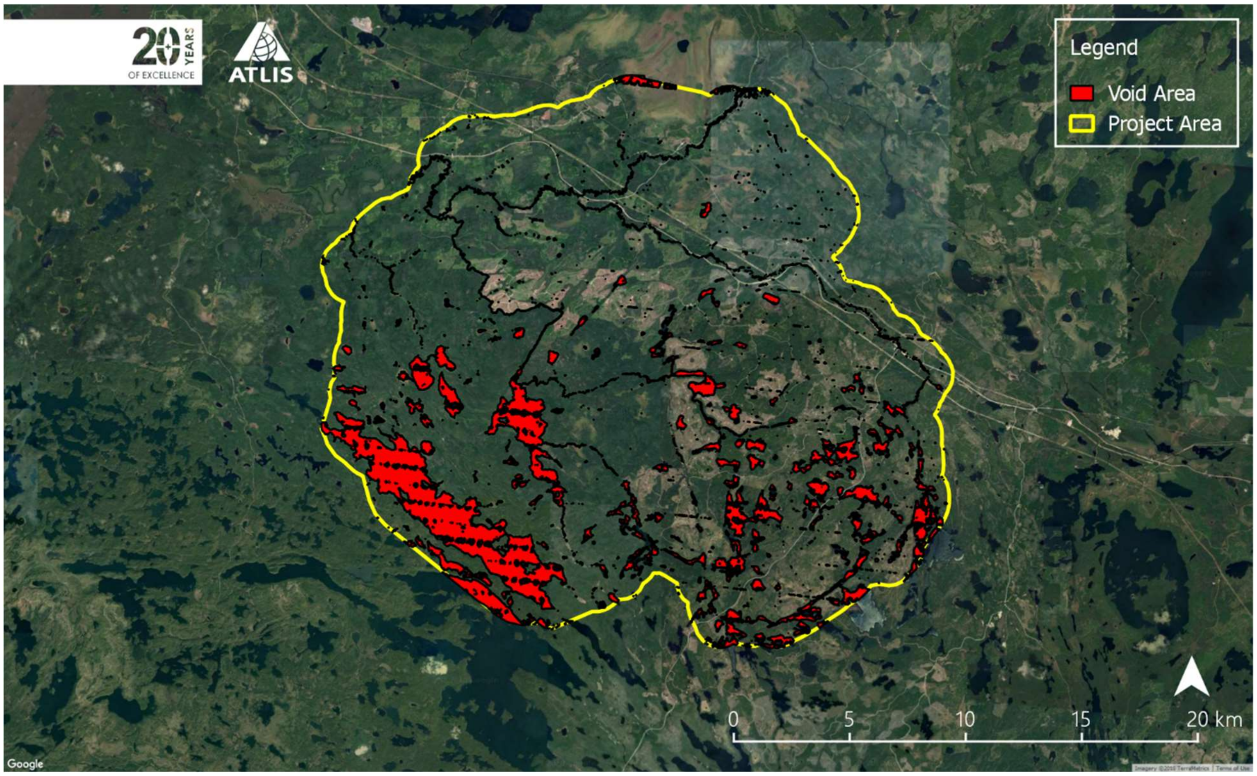

Figure 13: Void Area Map

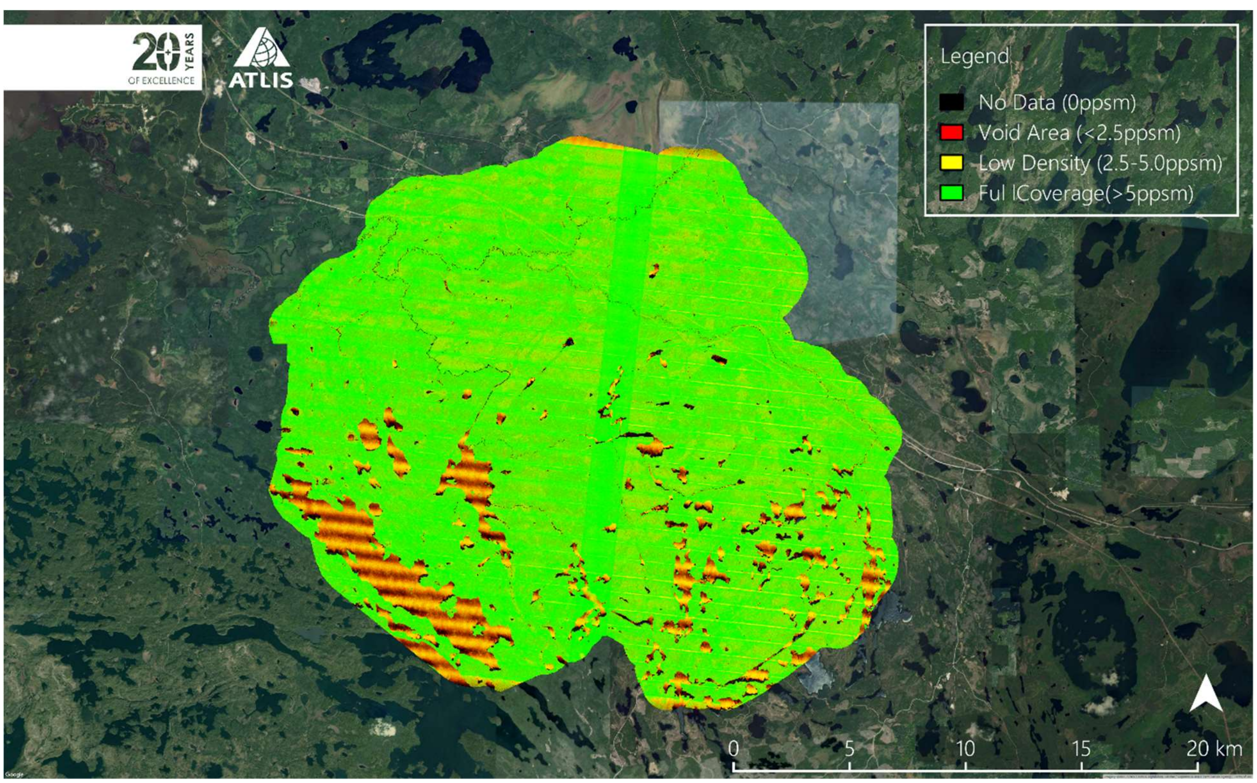

Figure 14: Density Map

4.4 CLASSIFICATION

ATLIS classified the LiDAR data using a series of macro-classification tools in TerraScan. The process for classifying the LiDAR starts by running a macro for isolated point, which are assigned to class 7 (Low Noise) and which are withheld from the final deliverable. Next, a ground macro routine is run to assign points to class 2 (Ground) from which a ground surface model is generated for further classification. ATLIS manual reviewed and re-assigned points to and from class 2 (Ground) to ensure that all appropriate points were correctly assigned to class 2 (Ground) and to assign points to class 9 (Water). The remaining points in class 0 (Never Classified), all those below the ground surface were assigned to class 7 (Low Noise) and all those above the ground surface were assigned to class 3 (Low Vegetation). A macro was then run on the points in class 3 to populate class 4 (Medium Vegetation) with all points greater than 30cm above the ground surface. The vegetation macro was then run again on class 4 Medium Vegetation) to populate class 5 (High Vegetation) with all points greater than 3m above the ground surface. And finally, a macro was run on class 4 (Medium Vegetation) to assign points to class 6 (Buildings).

Table 13 shows the break-down of how the LiDAR points for this project were classified.

CLASS	DESCRIPTION	NO. OF POINTS	PERCENTAGE
0	Created, never classified	0	0.0%
1	Unclassified	0	0.0%
2	Ground	613,743,939	14.9%
3	Low Vegetation	1,054,008,063	25.6%
4	Medium Vegetation	534,018,082	13.0%
5	High Vegetation	1,847,679,052	44.9%
6	Building	11,344	0.0%
7	Low Point (noise)	0	0.0%
8	Model Key-point (mass point)	0	0.0%
9	Water	62,592,028	1.5%
	TOTAL	4,112,052,508	100%

Table 13: LiDAR Classification Break-down

4.5 SURFACE MODELS. CONTOURS AND HILLSHADE

SURFACE MODELS

ATLIS generated a bare-earth Digital Elevation Model (DEM) from the class 2 (Ground) LiDAR data and a first-return Digital Surface Model (DSM) from the LiDAR points classified as first-return (excluding class 7) using ArcGIS. Elevations were computed on a 1m grid by interpolating from a Triangulated Irregular Network (TIN) generated from the appropriate point cloud using the natural neighbor's method.

CONTOURS

ATLIS generated contours for this project from the ground classified LiDAR data using GeoCue LP360. The contours were generated at an interval of 0.5m and indexed at 2.5m using the required engineering method, no smoothing applied. The American Society for Photogrammetry and Remote Sensing (ASPRS) recommends a minimum contour interval of 3*$RMSE_z$, 0.084m in the case of this project. The contours generated for this project meet the contour interval recommendations of the ASPRS.

HILLSHADE

ATLIS generated the hillshade models for this project in Blue Marble Geographic Global Mapper using the classified LiDAR data, both bare-earth and first-return. Both hillshade models were generated using a 0° azimuth (north) and 60° altitude illumination parameters. The models were exported as 1-band, 8-bit TIFF rasters without compression.

4.6 ACCURACY

The National Standard for Spatial Data Accuracy (NSSDA) published by the Federal Geographic Data Committee (FDGC) defines the vertical accuracy of a LiDAR dataset as:

$$RMSE_z = \sqrt{\sum \left(Z_{data,i} - Z_{check,i}\right)^2 / n}$$

The Vertical Accuracy for the LiDAR data of this project was determined to be 0.025m $RMSE_z$ and 0.049m at the 95% confidence level, based on the eleven check points used. The acceptance criteria for the vertical accuracy of this project is 0.075m $RMSE_z$ and 0.150m at the 95% confidence level.

The National Standard for Spatial Data Accuracy (NSSDA) published by the Federal Geographic Data Committee (FDGC) defines the horizontal accuracy of a LiDAR dataset as:

$$RMSE_r = \sqrt{\sum \left(\left(x_{data,i} - x_{check,i}\right)^2 + \left(y_{data,i} - y_{check,i}\right)^2\right) / n}$$

None of the check points surveyed by ATLIS for this project are conducive to this accuracy specification.

The Leica Brochure for the ALS70 states that the estimated horizontal accuracy at nadir and at an above ground height of 1550m is approximately 14cm $RMSE_r$ or 27cm at the 95% confidence level, as shown in *Figure 15*. The horizontal accuracy acceptance criteria for this project is 30cm.

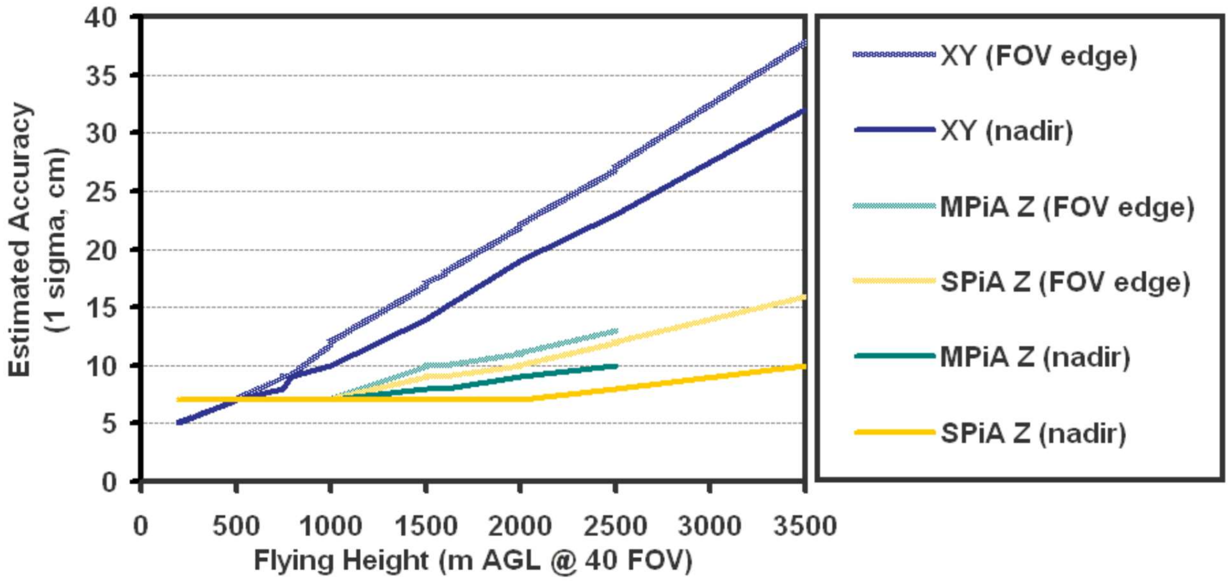

Figure 15: Manufacturer Estimated Accuracy of the ALS70

CATEGORY	DESCRIPTION	NO. OF POINTS	$RMSE_Z$
1	Bare-earth and low grass (plowed fields, lawns, and golf courses)	11	0.025m
2	High grass, weeds, and crops (hay fields, corn fields, and wheat fields)	0	-
3	Brush lands and low trees (chaparrals, mesquite)	0	-
4	Forested, fully covered by trees (hardwoods, evergreens, and mixed forests)	0	-
5	Urban areas (high, dense manmade structures)	0	-
6	Sawgrass	0	-
7	Mangrove	0	-

Table 14: Ground Cover Categories

5.0 ORTHOPHOTO PROCESSING

Initial recovery of the raw image frames was performed by Eric Gareau using Leica FramePro using the setting outlined in *Table 15*.

Color Saturation	1.80	**Bits Per Band**	8
Gain	10.03	**Band Combination**	RGBN
Gamma	2.62	**Format**	Tiff

Table 15: Image Recovery Settings

The Aerial Triangulation (AT) of the aerial imagery was performed by Eric Gareau using Trimble Inpho to compute the External Orientation (EO) parameters of the image frames. The ortho-rectification, ortho-mosaicking and seamline editing tasks for this project were performed by Weaverbird Engineering & Technology. The final orthophoto quality checks were performed by

The processed aerial orthophoto was produced at a 20cm resolution in 4 bands (RGBN) with a bit-depth of 8bit per channel. ATLIS tiled the orthophoto into 1000m x 1000m tiles saved as GeoTIFF files, with each tile named according to the UTM coordinate in the southwest corner of the tile.

5.1 AERIAL TRIANGULATION

ATLIS computed the External Orientation (EO) parameters for all 1667 photos captured for the project using an Aerial Triangulation (AT) process in Trimble Inpho by Eric Gareau. The process generated a total of 544,494 measurements to create 1,093,647 observations, which were used to solve for 481,704 unknowns, providing a redundancy of 611,943.

Figure 16 shows the number of points generated that connect a given number of photos and *Table 16* shows the RMS values for the various classes of points used in the AT process. *Table 17* summarizes the standard deviation statistics for the EO parameters computed from the AT process.

ATLIS computed coordinates for each of the Ground Control Points (GCPs) using multiple stereo photos for comparison with the coordinates derived from the ground survey. Because ATLIS was unable to access most of the project site, a point was computed from the LiDAR data at the corner of the waterbody, shown in *Figure 17*, to serve as a third GCP for the aerial survey. The measurement residuals from the AT process to the surveyed coordinates of the GCPs is shown in *Table 18*.

The RMSE of known GCPs is demonstrated to be significantly lower than the required 0.285m required for this project, as illustrated by *Table 16*.

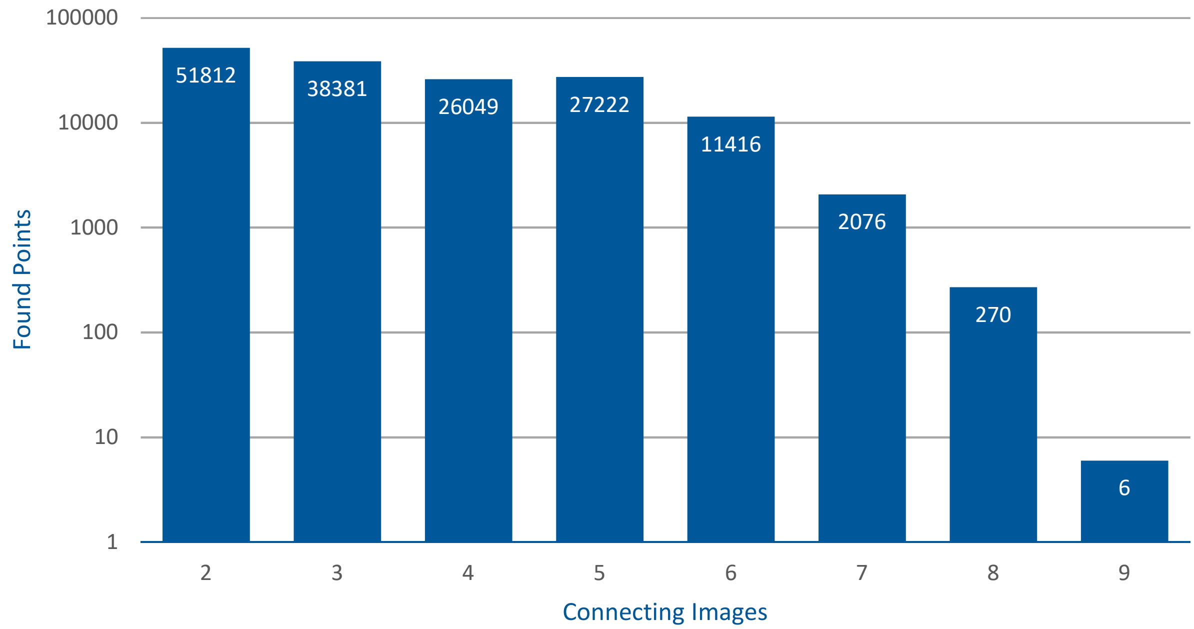

Figure 16: Found Points Connecting Photos

RMS CLASS	NO. OF POINTS	X	Y	Z
Automatic Points	542,167	1.4µm	1.4µm	-
Control and Manual Points	2,148	2.6µm	1.5µm	-
Control Points with Default σ	2	0.019m	0.003m	-
Control Points with Default σ	10	-	-	0.001
Control Points with σ set 1	1	0.096m	0.014m	-
Control Points with σ set 1	0	-	-	0.000m
GNSS Observations	1667	0.114m	0.074m	0.071m

Table 16: RMS values for AT Points

	OMEGA(MDEG)	PHI(MDEG)	KAPPA(MDEG)	X(M)	Y(M)	Z(M)
Mean σ	1.5	1.5	1.4	0.041	0.046	0.076
Max σ	5.2	5.6	14.6	0.043	0.048	0.081

Table 17: Standard Deviations of Exterior Orientation Parameters

CONTROL POINT	ΔX	ΔY	ΔH	ΔZ
STATIC001	0.027	-0.005	0.027	0.002
STATIC002	0.002	0.000	0.002	0.001
LIDAR1	-0.096	0.014	0.097	-0.001
Average	-0.022	0.003	0.042	0.001

Table 18: AT Control Point Residuals

Figure 17: Synthetic Ground Control Point LIDAR1

5.2 ORTHOPHOTO GENERATION

ATLIS contracted Weaverbird Engineering & Technology to produce the orthophoto for this project. Weaverbird ran an ortho-rectification process on the photos using a combination of the EO parameters estimated in the AT process and a bare-earth surface model generated from the classified LiDAR data to remove the effect of perspective from the imagery.

Weaverbird then combined the ortho-rectified images to produce an ortho-mosaic and radiometrically adjusted the ortho-mosaic to produce an orthophoto that was radiometrically consistent across the entire project area. Weaverbird performed manual seamline edits on the ortho-mosaic to remove any unwanted artifacts and reduce alignment errors around the seamlines.

ATLIS reviewed Weaverbird's work product to ensure that the resulting orthophoto met the quality requirements for this project. The orthophoto quality control checks were performed by Neel Chooniedass.

5.3 ACCURACY

The National Standard for Spatial Data Accuracy (NSSDA) published by the Federal Geographic Data Committee (FDGC) defines the horizontal accuracy of a given point (i) in an image as:

$$\sqrt{\left(x_{data,i} - x_{check,i}\right)^2 + \left(y_{data,i} - y_{check,i}\right)^2}$$

And the horizontal RMSE as:

$$RMSE_H = \sqrt{\sum\left(\left(x_{data,i} - x_{check,i}\right)^2 + \left(y_{data,i} - y_{check,i}\right)^2\right)/n}$$

POINT	ΔX	ΔY	ΔR	ACCEPTANCE CRITERIA
STATIC001	0.027	-0.005	0.027	-
STATIC002	0.002	0.000	0.002	-
LIDAR1	-0.096	0.014	0.097	-
RMSE	0.058	0.009	0.058	0.100
95% Confidence (1.2239*($RMSE_x$ + $RMSE_y$))			0.082	0.200

Table 19: RMSE and Acceptance Criteria for Orthophoto Control Points